

Tunnelling effects and electron transport in quantum dot structures

L. Pichl^{a,1}, J. Horáček^b, V. Mitin^c, V. Ryzhii^a

^aUniversity of Aizu, Tsuruga, Ikki, Aizu-Wakamatsu, 965-8580, Japan

^bInstitute of Theoretical Physics, Charles University Prague, V Holešovičkách 2, Praha 8, 180 00, Czech Republic

^cWayne State University, Detroit, Michigan, 48202, USA

Abstract

Using an analytical model of electron confinement in quantum dots, we have calculated the tunnelling rates for electron quasi-bound states. Schrödinger equation for the disk-shaped system in consideration is readily solved both in the time-dependent and time-independent versions, and the quantitative importance of tunnelling phenomena in low temperature electron emission from quantum dots is revealed. Results of the quantum mechanical analysis are transferred into the device characteristics of common multi-layer quantum dot hetero-structures.

Key words: Quantum dot; Tunnelling rate; *QD* energy levels; Wave packet dynamics; Axial symmetry

Introduction

It is generally recognized that the properties of multi-layer quantum dot (*QD*) devices, such as photodetectors, critically depend on the number N of electrons occupying the *QD*, and the electron capture/emission rates. This is because the electric current under applied voltage, $j \sim e \frac{\Sigma_{QD}}{p} G$, is proportional to the electron escape rate, $G = G(N)$ (due to photo-induced, thermionic or any other mechanism), density of *QDs*, Σ , and inversely proportional to the electron capture probability, $p = p(N)$.

The thermal dark current and photocurrent in *QD* structures have been studied in detail previously [1]. However, for the calculations of the dark current characteristics at low temperatures, the explicit dependence of the electron tunnelling escape rate on N and other parameters is indispensable. Specific features of *QDs* studied in the recent experiments are low *QD* density Σ_{QD} and a flattened shape. This provides the possibility of spontaneous electron tunnelling in the lateral directions when *QDs* are markedly charged.

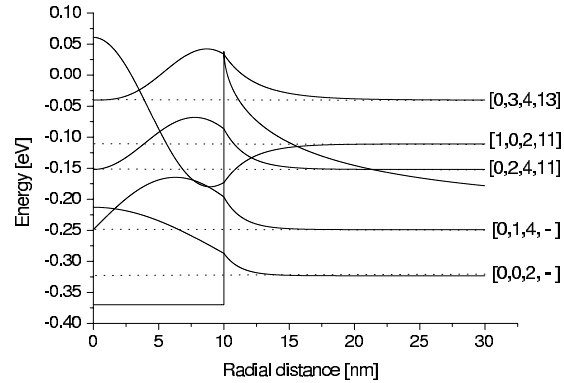


Fig. 1. Schematic view of *QD*. Bold line: the potential curve ($N=16$, centrifugal terms excluded). Dotted lines: energy levels, thin lines: wave functions (arbitrary units). Numbers in bracket indicate: [quantum numbers n, m , maximum level occupation number, and minimal N for which tunnelling may occur].

Model Quantum Dot

Let us review a typical *QD* in hetero-structures considered above. The important *QD* parameters are especially (i) the lateral radius, a , (ii) the thickness of *QD*, l , (iii) the confinement potential V_{QD} (conduc-

¹ Corresponding author (present address as above).
FAX: +81-242-37-2734, E-mail: lukas@u-aizu.ac.jp

tion band offset), (iv) dielectric constants, κ , κ_{QD} (v) electron masses μ , μ_{QD} , and (vi) the total confined charge N . The 2D axially symmetric hamiltonian is

$$\hat{H} = -\frac{\hbar^2}{2\mu_i} \left[\frac{\partial^2}{\partial r^2} + \frac{1}{r} \frac{\partial}{\partial r} - \frac{m^2}{r^2} + \frac{\partial^2}{\partial z^2} \right] + V(r, z), \quad (1)$$

where m is the azimuthal quantum number. Let us invoke the flat disk quantum dots, assuming only one quantum level in the z -direction, $l_{QD} \ll a$. Supposing further a QD with a number of electrons (thus closer to a uniform charge distribution), the z -dimension may be reduced out, and the potential function $V(r, z) \simeq V(r)$ includes both the QD attraction and electrostatic repulsion,

$$V(r) \simeq \begin{cases} -V_0 & \text{for } r \leq a, \text{ and otherwise:} \\ Z \frac{e}{a} \left[\frac{1}{\kappa} \arctan \left(\sqrt{\frac{a^2}{r^2 - a^2}} \right) - \frac{\pi}{2\kappa_{QD}} \right] & \end{cases} \quad (2)$$

This potential is shown in Fig. 1 for $N = 16$.

Results and Discussions

The n -th bound-state wave function of single electron,

$$J_m \left(\sqrt{2\mu_{QD}(E_n - V_0)} r / \hbar \right) \text{ for } r \leq a, \quad (3)$$

$$H_m^{(1)}(i\sqrt{2\mu(-E_n)}r/\hbar) \text{ for } r \geq a, \quad (4)$$

is to be matched numerically at $r = a$. The ratio of logarithmic derivatives between the Bessel and Hankel functions [2] is prescribed as μ_2/μ_1 , which yields the energy spectrum, $\{-|E_n|\}_n$. The electrostatic potential in Eq. (2) is a perturbation, which effectively lowers the the confinement potential at large r . The energy levels $E_n > -Ne\pi/(2a\kappa_{QD})$ thus become open for tunnelling (cf. Fig. 1). The tunnelling rates are then obtained by solving the time-dependent Schrödinger equation with the initial wave packet given by Eq. (3), for which several time-space grid method or the split-operator technique can be employed. We adopt the Vischer al-

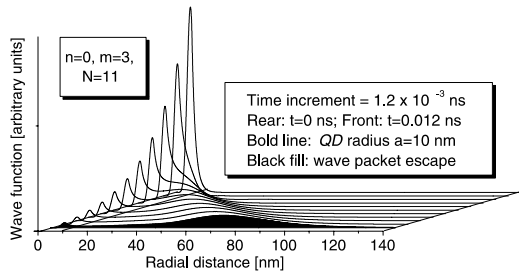


Fig. 2. Tunnelling dynamics in time.

gorithm, since it is sufficiently fast and also unitary. Absorbing boundary condition is implemented (i.e., a

small negative imaginary part added to V at large values of r). Invoking the well studied InAs/GaAs QD system, let us choose the typical QD parameters $a = 10$ nm, $\kappa_{QD} = 15.15$, $\kappa = 12.91$, $\mu_{QD} = 0.027m_0$, $\mu = 0.067m_0$, $V_{QD} = 0.37$ eV and $N = (0 - 16)$. Energy levels follow from Eq. (3), results are shown in Fig. 1. For each level k , the population number $0 \leq \nu_k \leq 1$ is time dependent, $\nu_k(t) = \int_{QD} |\psi_k(r, t)|^2 dr$, with $\nu_k(t) \simeq \exp(-\lambda_k t)$. The tunnelling rates λ_k (in ns^{-1}):

N	11	12	13	14	15	16
$n=0, m=2$	0.01	0.20	1.03	2.73	5.88	11.5
$n=1, m=0$	72	101	131	162	195	222
$n=0, m=3$			389	432	476	519

The total tunnelling rate reads $-dN(t)/dt|_{t=0} = \sum_k N_k \lambda_k$, where N_k is the number of electrons occupying the k th level. In Fig. 3, the total tunnelling rate as a function of charge N is displayed (the above InAs/GaAs QD parameters were used). The increase

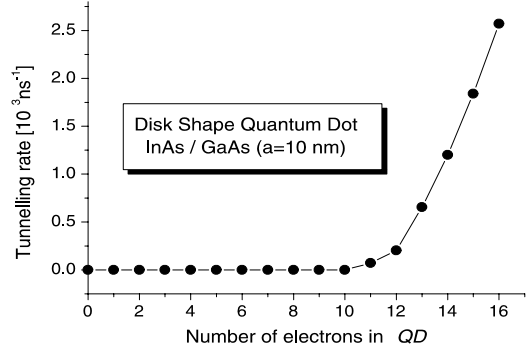


Fig. 3. Electron total tunnelling rate as a function of charge

in the tunnelling rate with N is due to two factors, (1) increase of the electron repulsion inside QD , and (2) occupation of higher lying QD states closer to the barrier top. The slope change in Fig. 3 from $N = 11, 12$ to $N = 13, \dots, 16$ is, e.g., due to a newly occupied level $n = 0, m = 3$ at $N \geq 13$ (cf. Fig. 1). Figs. 1, 3, and the state-resolved tunnelling rate tables are the main results used in low temperature device models.

Acknowledgments

L.P. would like to thank JSPS for the support by Grant-in-Aid 21602/13/01073.

References

- [1] V. Ryzhii, *Semicond. Sci. Technol.* 11 (1996) 759.
- [2] M. Abramowitz and I. Stegun, *Handbook of Mathematical Functions* (Dover, New York, 1972).